SATELLITE OBSERVATIONS WITH A SINGLE RADAR TRACKING STATION

D. Mehrholz

Research Institute For High Frequency Physics (FHP)
Research Establishment For Applied Science (FGAN)
Wachtberg-Werthhoven
Germany

ABSTRACT

The observation of earth orbiting satellites by use of one radar tracking station only is discussed. Handicaps in observations due to the relative motion between a satellite and the radar station are highlighted. Based on the assumption that decaying high-risk space objects have to be observed, some basic radar system requirements are defined. Experiences gained during the employment of a Satellite Acquisition And Tracking Radar for purpose of re-entry surveillance of space debris are discussed.

Keywords: Observation of Decaying Space Objects, Earth Orbiting Satellites, Radar Tracking, Radar System Requirements.

1. INTRODUCTION

Detection of space objects using radio frequencies below 20 GHz are usually not hampered by atmospheric influences due to the excellent allweather performance of radar systems. Clutter is also not a problem. In contrast to optical systems the employment of a radar station is basically limited only by the observation scenario satellite/radar station and by the overall radar power budget.
Radar observations usually do not presume a target cooperation, however, targets must reflect electromagnetic energy.
In order to gain information about target characteristics, it is not sufficient to take a snapshot only. The target has to be tracked during the entire passage by the radar.
There are many solutions available to solve radar surveillance tasks, and systems have been built to fit special requirements for search or tracking (Refs. 1, 2). However, for purpose of this report, a monopulse type radar supported by a mechanical movable antenna dish with pencil beam characteristic is assumed (Refs. 3,4).

2. INFORMATION FROM RADAR RETURNS

2.1 Information Available

The transmitted electromagnetic energy of the radar is scattered from the target, and all data which a radar sensor can gain are contained in the electromagnetic field.
Directly available from radar measurements are range, relative velocity, angular direction, and echo amplitude. For certain applications the radar should have the capability for phase and polarization measurements too. Using mathematical algorithms additional target characteristics can be calculated like: target trajectories, size, shape, intrinsic motion, and perhaps vibration. Comparing results from more than one observation period some more information can be gained: maneuver capability, fragmentation, life time, and target mass.

2.2 Information Needed

Radar observations of decaying, non-cooperative, high-risk space objects should gain data to determine:

- o actual orbital elements, and
- o target characteristics.

Space objects at low altitudes (less than 200 km) are characterized by fast changing orbital elements. Highly actual orbital elements of excellent accuracy are needed to prepare the next observation, to forecast ground tracks, and to predict object's life time (Ref. 5). Therefore as many passages as possible must be observed to gain reliable radar data. Angular direction measurements or range measurements are sufficient to calculate orbital elements. In many cases a combination of those data supported sometimes by Doppler frequency measurements (relative velocity) are used.
Target characteristics like the intrinsic motion, dimensions of simply shaped bodies, and mass can be determined from echo amplitude measurements (Ref. 6). If the target structure is more complex and knowledge of more target details is required, echo amplitude, echo phase, and echo polarization should be measured.

3. OBSERVATION SCENARIO

The observation scenario is characterized by the following features:

- o Single ground based radar tracking station,
- o mechanical movable antenna dish, and
- o monopulse type radar.

3.1 Single Radar Tracking Station

It is obvious that for purposes of radar observations employing a ground based station, the target must be at line-of-sight with respect to the radar station (Figure 1).
Assuming nearly circular orbits, less then 10 % of one orbit can be observed (Figure 2).

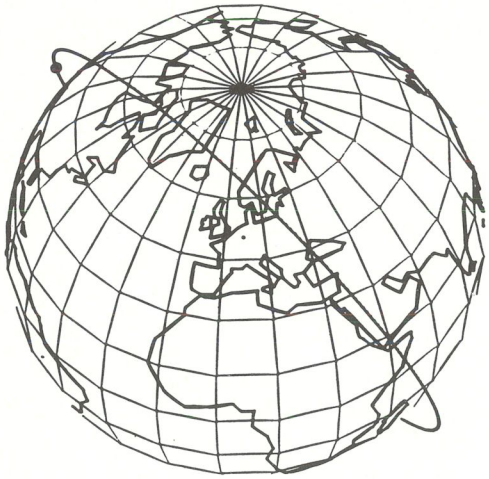

Figure 1. Radar Observation Scenario

The relation between satellite altitude h, slant range D, and maximal observation time B is shown. Parameter is the elevation angle e under which the target enters and leaves the observation window.

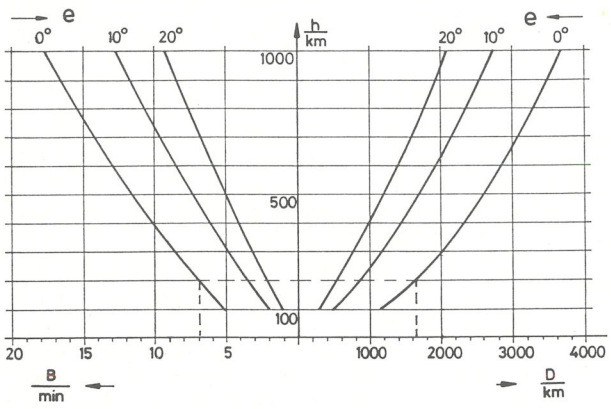

Figure 2. Maximal Observation Time B and maximal Slant Range D as Function of Satellite Altitude h and Elevation Angle e, under which the Target enters and leaves the Observation window (Circular Orbit).

The situation for an object at 200 km altitude is marked. Detection at the horizon (0^{o} elevation) will happen in 1700 km distance and it takes 7 minutes until the passage is completed. Should the target be first detected at higher elevation angles, the detection range and time for observation are much shorter.
Dependent on object orbit altitude, only up to 8 orbits per day (50 %) are visible. Figure 3 shows the situation for the US radar calibration satellite RADCAT. On the X-axis day numbers per year are plotted and on the Y-axis hours per day. Observation intervals are presented at the correct scale. Useful radar data are gained from at best 6 orbits per day since radar measurements at low elevation angles (less than 5 degrees) are too much disturbed by atmospherics. Low passages with object detection only might be needed to test whether the object is still orbiting.
Figure 3 shows also that breaks of about 8 hours and 5 hours between consecutive observations are possible. In a worst case situation a total loss of radar data for about 14 hours must be taken into account.

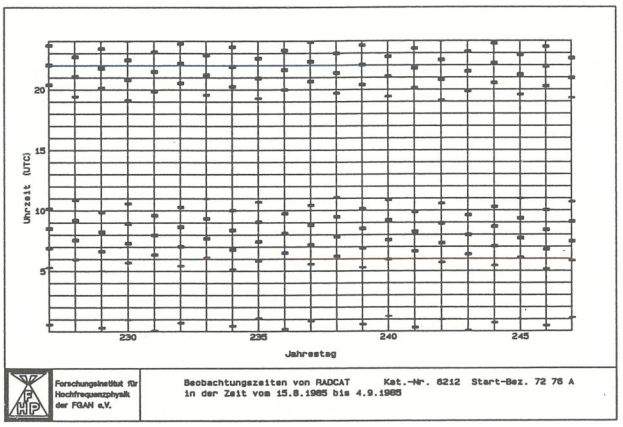

Figure 3. Observation Intervals of the Radar Calibration Satellite RADCAT.

This situation can be critical as shown in chapter 5, especially if the observed object is going to decay short time before or after such break periods. It is well known that life time predictions based on relatively old radar data are unreliable.

3.2 Mechanical Movable Antenna Dish

The observation of a satellite passage starts usually with an azimuth scan at pre-calculated coordinates, where the object is expected to cross the horizontal plane. After completion of the acquisition phase, tracking is activated. The antenna dish is moving in azimuth and elevation axis with increasing speed. Assuming circular orbits, maximal azimuth speed is evolving when elevation culminates. Passages where the satellite is passing the radar station nearly overhead (culmination at more than 85 degree elevation) are critical. In such cases, azimuth speed of more than 30 degree/sec are easily exceeded.
Although assuming a highly engineered azimuth/elevation pedestal mount, restrictions in the observation due to the mechanical movableness have to be taken into account. Areas can be specified where tracking quality is degraded or where tracking is completely lost.
Another implication is the relation between antenna dish size and antenna beam width. Employing a large antenna results in a pencil beam which makes preknowledge about object orbit necessary.

3.3 Type of Radar

For purpose of this report, a monopulse type radar with a modern signal processing concept is assumed. But, nevertheless, the radar observation volume is limited by the radar power budget (determines maximal detection range for a given target size) and by the transmitted pulse length (1 msec pulse length results in 150 km blind area at least). Radar peak power and pulse length are trade-offs. They are chosen in conjunction with the signal processing concept to solve the radar energy problem.

4. RADAR SYSTEM REQUIREMENTS

Design of radar systems requires assumptions about the radar cross section (RCS) of the target and the maximal detection range. If decaying high-risk

objects have to be observed, the figures listed in Table 1 are relevant.

Table 1.

High-risk decayed Objects	RCS L-Band (dBsm)	Range minimal (km)	Range maximal (km)
SKYLAB 1	0 to 50	150	2400
RORSAT	-10 to 30	150	1800
RORSAT Core	-20 to -3	150	1700

Based on these values, requirements can be developed for:

- o mechanical movableness of the antenna,
- o radar transmitter power,
- o radar signal processing scheme, and
- o antenna size.

In order to give the reader a feeling about some basic radar system requirements, the mechanical movableness of the antenna dish and the relation between antenna size and transmitted radar power is discussed.

4.1 Mechanical Movableness

For large antenna dishes (more than 10 m diameter) designers prefer the horizontal mounting (one axis perpendicular to the horizontal plane) rather than the equatorial mounting (one axis perpendicular to the equator plane). The second axis is in both cases rectangular mounted to the first axis. The control of the total mass (hundreds of tons for a 30 m dish) of the antenna construction is easier to achieve having a horizontal mounting. Therefore, it is assumed that the radar is supported by an azimuth/elevation pedestal.
If space objects with orbit inclination angles larger than the geographical latitude of the radar station have to be observed, then the antenna dish should be movable in azimuth by ± 360 degree and in elevation from 0 to 90 degree at least.
Figure 4 shows the maximal speed needed in azimuth and elevation axis during the observation of the entire passage of an orbiting object as function of the culmination angle E. Parameter is the satellite altitude h.

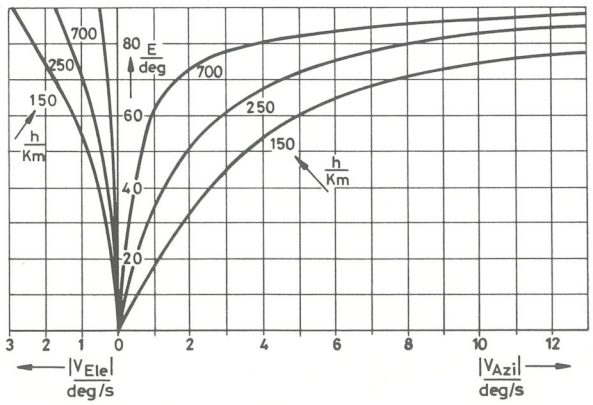

Figure 4. Maximal Speed in Azimuth and Elevation Axis as Function of Culmination Angle E and Satellite Altitude h.

4.2 Antenna Size Versus Radar Power

The outside world of a radar system is described by Eq. 1 (Ref. 1). The first fraction of this equation describes the power density at distance R, if power P_t is transmitted with an antenna having G_t antenna gain (Figure 5).

$$P_r = \frac{P_t * G_t}{4*pi*R^2} * \frac{RCS}{4*pi*R^2} * A_r * \frac{1}{L_t} * \frac{1}{L^2_{at}} * \frac{1}{L_r} \quad (1)$$

The power density at distance R multiplied with the RCS of the target gives the amount of power which is backscattered to the radar. The product of the first two fractions is the power density at the receiving radar antenna. Multiplication with the receiving antenna aperture A_r results in the received power P_r. For a real situation this value must be diminished by losses L due to transmitter, atmospheric, and receiver paths.

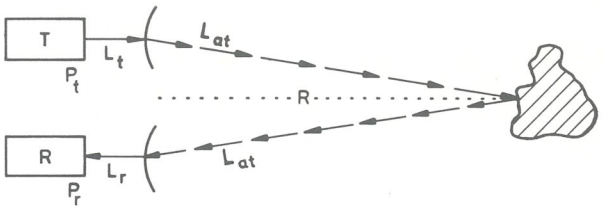

Figure 5. Illustrating the Radar Power Budget

The inside world of the radar system is described by Eq. 2 (Ref. 1):

$$P_r = S/N * k * T_o * F_N * B \quad (2)$$

The received power P_r necessary to process the information contained in the radio signal is a function of the signal to noise ratio S/N, the receiver noise figure F_N measured at reference temperature T_o, and the processed bandwidth B. The factor k is the Boltzmann figure.
Equalizing Eq. 1 with Eq. 2 and assuming that the same antenna with the diameter D and the efficiency eta is employed for transmission and reception, and introducing the wavelength wl of the radar frequency used, the Eqs. 3.1-3.3 evolve:

$$P_t*(D^2/wl)^2 = const, \quad (3.1)$$

$$const = \frac{64}{pi*eta} * S/N*k*T_o*F_n*B*R^4* \frac{1}{RCS} * L, \quad (3.2)$$

$$L = L_t * L^2_{at} * L_r. \quad (3.3)$$

Figure 6 shows at the right hand part graphically the situation described by Eq. 3.1. Using half-

Table 2

Value	Figure	Remarks
S/N	10 dB	Acquisition and tracking
F_N	2 dB	Inclusive limiters, comparator, and receiver
B	3 kHz	Correlation and filtering
eta	50 %	Antenna efficiency
R	1700 km	RORSAT Core (see Table 1)
RCS	-20 dBsm	RORSAT Core (see Table 1)
L_t	0.2 dB	Waveguides, rotary joints, power divider etc
L_{at}	2 dB	L-Band
L_r	1 dB	incl. Radome attenuation

logarithmic scale the relation between antenna dish diameter D and the transmitted radar power P_t necessary to track a decaying high-risk space object like the RORSAT core is presented. The left hand part of Figure 6 shows the relation between antenna dish diameter D and the 3 dB antenna beamwidth theta. Table 2 summarizes essential assumptions (some of which are given in dB) for the processing of Eqs. 3.1-3.3.

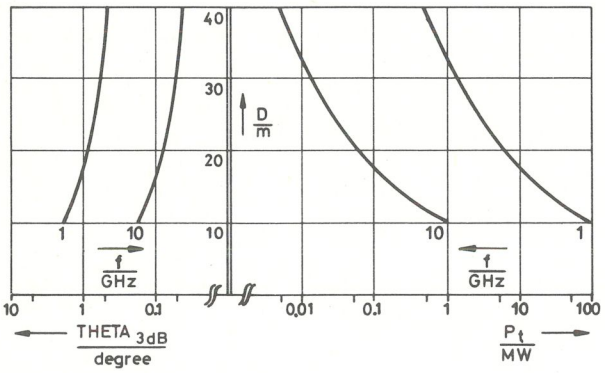

Figure 6. Antenna Dish Diameter D as Function of the transmitted Radar Power P_t and 3 dB Antenna Beamwidth theta. Parameter is the Radar Frequency f (Additional Assumptions see Table 2).

5. EXPERIENCES GAINED

The High Power Radar Systems Division (GA) of FHP deals with the design, realization, and operation of radar systems for surveillance and reconnaissance tasks. For purpose of space object identification FHP/GA developed a Satellite Acquisition And Tracking Radar (SATRA) (Refs. 7, 8). The aim is to investigate scientific and technical problems in the area of long distance radar surveillance.
Ordered by the Minister Of Interior (MOI) Germany, SATRA was employed for the surveillance of decaying high-risk space objects as listed in Table 3.

Table 3

Object Name	Decay Date DD.MM.YYYY	Time (GMT) HH:MM
COSMOS 954	24.01.1978	11:55
SKYLAB 1	11.07.1979	16:29
COSMOS 1402 A	23.01.1983	22:21
COSMOS 1402 C	07.02.1983	11:07

After decay of COSMOS 954 the MOI Germany organized a Bund/Länder-Working Group to develop recommendations and procedures how to handle best such incidents. The findings were tested during the decay observation of SKYLAB 1 (Refs. 9, 10) and improvements, especially in the area of information and data distribution, were realized. Figure 7 shows the information network and organizations involved in the re-entry predictions of COSMOS 1402.
Two radar observations in the re-entry phase of COSMOS 1402 A and C have been selected to highlight the situation. At first Figure 8 shows the observation intervals of COSMOS 1402 A for the last 20 days.
Because of the orbit situation, there are breaks of about 14 hours between two consecutive observations. The last passage measured at 17:22 hours (GMT) is indicated. A passage at low elevation follows where the object was detected by the radar, but useful radar data could not be obtained. Approximately three hours later there was another low elevation passage where only detection was possible. The decay happened some 20 minutes later at 22:21 (GMT). Assuming ±10 % accuracy in life time prediction, the uncertainty would have been ±30 minutes if the prediction was performed a short time after and based on the last observation.

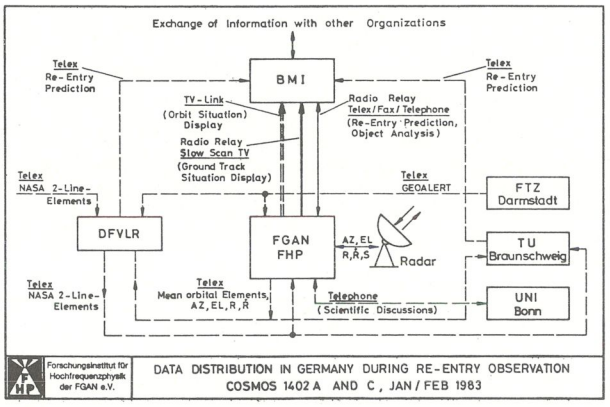

Figure 7. Distribution of Information and Data during the Re-Entry Predictions of COSMOS 1402 A and C and Organizations involved in January and February 1983.

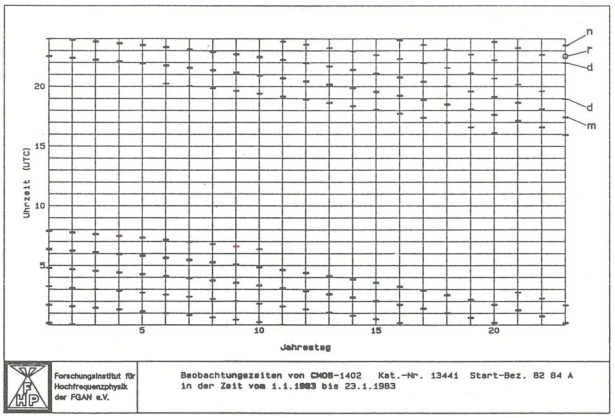

Figure 8. Observation Intervals of COSMOS 1402 A (Recorded from 1 to 23 January 1983).

m: last orbit measured at 17:22 (GMT),
d: object detected only at 18:56 and at 21:59 (GMT),
r: re-entry at 22:21 (GMT),
n: next calculated possible passage at 23:27 (GMT).

The next Figure 9 shows a summary of radar data from the last passage measured.
The amplitude plot as function of time shows that the object was tumbling with a rate of approximately 24 sec. The Doppler frequency (relative velocity) is measured as function of time in kHz with respect to L-Band radar frequency. The polar plot shows the observation scenario with respect to the angular direction in azimuth (AZI) and elevation (ELE). Tracking was activated at X, * marks the point of closest approach. Although the culmination of elevation was only 14.7 degree, the radar data measured were of high quality.

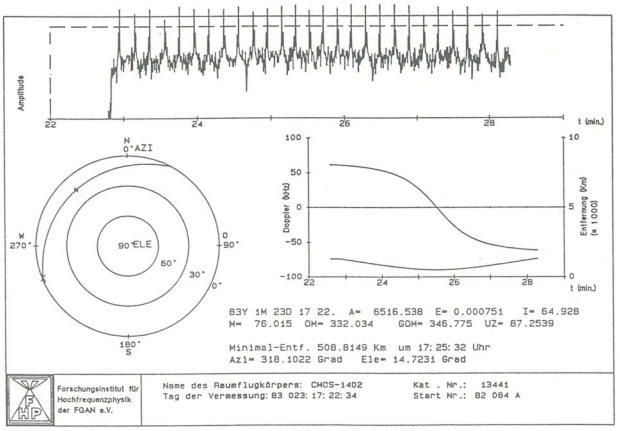

Figure 9. Radar Data measured from COSMOS 1402 A on the last Passage at 23 January 1983.

With Figure 10 the observation intervals of COSMOS 1402 C are displayed. The worst case situation as discussed in chapter 3.1 happened.

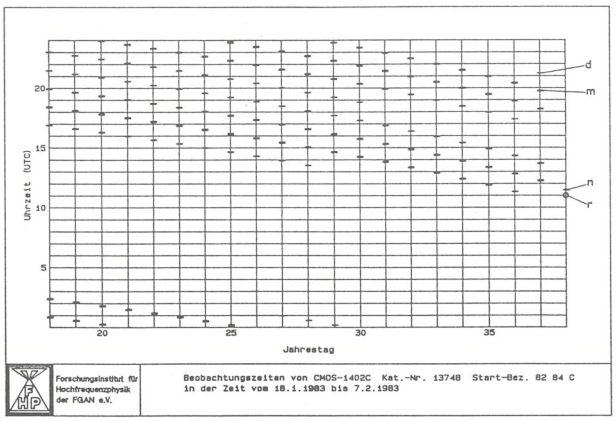

Figure 10. Observation Intervals of COSMOS 1402 C (Recorded from 18 January to 7 February 1983).

m: last orbit measured at 19:40 (GMT),
d: object detected only at 21:12 (GMT),
r: re-entry at 11:07 (GMT),
n: next calculated possible passage at 11:25 (GMT).

While the object was measured during the passage at 19:40 hours (GMT) (Figure 11), the consecutive passage could only be detected because of low elevation. The decay was on the next day at 11:07 hours (GMT); that was approximately 14 hours after the last detection and more than 15 hours after the last radar measurements. Life time prediction, based on the measured radar data, would have had ±90 minutes accuracy which are more than two revolutions.
The last Figure 11 highlights the problem which has been discussed at chapters 3.2 and 4.2. The last passage was a overhead passage. Tracking was lost due to limitations in mechanical movableness in the azimuth axis. The object was picked up again and tracked until it was lost at the end of line-of-sight.
The 14 hours breaks between two consecutive passages can cause total target loss if one operates a single radar station with pencil beam characteristic and if one misses highly actual data. This is especially true some days before object decay, when the orbital elements are changing fast, and the acquisition process (target detection and locking radar control loops) has to be based on old data. There is no difference whether these data are radar data, obtained 14 hours ago from the last observation, or old NASA 2-Line-Elements.

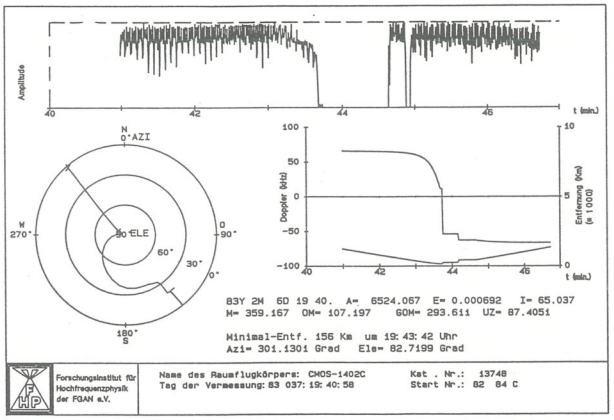

Figure 11. Radar Data measured from COSMOS 1402 C on the last Passage at 7 February 1983.

Because of the observation scenario outlined in this report, it would be desirable to have cooperation with other organizations which operate observation stations preferably in other parts of the world.

6. SUMMARY

Decaying high-risk space objects can be observed by use of a single radar tracking station only. But due to the scenario less than 10% of an orbit and 50 % of all orbits per day are within line-of-sight of the radar station. Breaks of about 14 hours between two consecutive passages are possible. This can cause total target loss because of outdated orbit data. Cooperation with other organizations, operating observation stations (in other parts of the world), is therefore desirable.
In order to fit the observation requirements like: orbit and groundtrack determination, life time prediction, dimension and mass assessment, the radar should deliver angular direction, range, and at least echo amplitude measurements.
For target detection and acceptable measurement errors the radar should transmit e.g. 1 MW peak power, pulse length approximately 1 msec, supported by a 30 m diameter antenna dish, assuming a state-of-the-art signal processing concept.
Mechanical movableness of the azimuth/elevation pedestal mount should be ±12 °/sec in azimuth and ± 2.5 °/sec in elevation. Angle area in azimuth should be ±360 degree and in elevation 0 to 90 degree at least.
Methods of exchanging information and data between communities of interest must still be improved, procedures for observation of decaying space objects must be trained.

7. REFERENCES

1. Skolnik M.I. 1970, Radar Handbook, McGraw-Hill, USA

2. Brookner E. 1977, Radar Technology, Artech House, Dedham

3. Mehrholz D. 1979, Voraussetzungen für den Einsatz der Großradaranlage des FHP und Darstellung von Erkenntnissen aufgrund gemessener Radardaten bei der Beobachtung von Risikoobjekten im Weltraum, FHP-Interner Bericht

4. Baars E.P., Mehrholz D. 1979, Radarverfahren zur Suche, Akquisition und Verfolgung von Satelliten, DGON, Symposium Radartechnik, Nov. 1979

5. Peters H.G. 1983, Auswertung von Satellitenbeobachtungen zur Bestimmung von mittleren Bahnelementen, FHP-Forschungsbericht Nr. 12-83

6. Gniss H., Magura K. 1982, Analyse von inkohärenten Radarsignaturen eines taumelnden, rotationssymmetrischen Satelliten, FHP-Forschungsbericht Nr. 7-82

7. Schäfer H. 1976, Systembeschreibung des Satellitenradars SATRA in Werthhoven, FHP-Interner Bericht

8. Pahls J. 1973, L-Band Monopuls Tracking Radar-(SATRA), FHP-Interner Bericht

9. Mehrholz D. 1978, Überwachung des Risikoobjektes SKYLAB-1, FHP-Interner Bericht

10. Mehrholz D. 1979, Meßtechnische Beobachtung der Raumstation SKYLAB-1, FHP-Interner Bericht